

## Metal–Ligand Cooperation in H<sub>2</sub> Production and H<sub>2</sub>O Decomposition on a Ru(II) PNN Complex: The Role of Ligand Dearomatization–Aromatization

Jun Li, Yoshihito Shiota, and Kazunari Yoshizawa\*

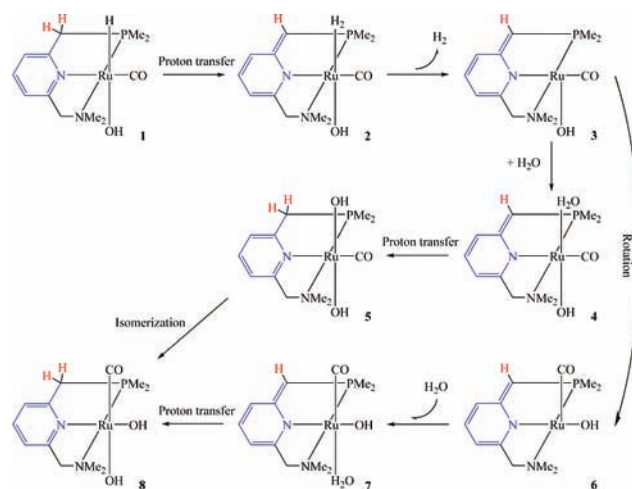
*Institute for Materials Chemistry and Engineering, Kyushu University, Fukuoka 819-0395, Japan*

Received June 20, 2009; E-mail: kazunari@ms.ifoc.kyushu-u.ac.jp

The sunlight-driven splitting of water into H<sub>2</sub> and O<sub>2</sub> is an attractive and challenging issue in science today.<sup>1</sup> Recently, Milstein's group achieved a distinct scheme in which H<sub>2</sub> and O<sub>2</sub> were generated in consecutive thermal- and light-driven steps.<sup>2</sup> Heating the monomeric aromatic Ru(II) hydrido–hydroxo complex [C<sub>5</sub>NH<sub>3</sub>(CH<sub>2</sub>P<sup>t</sup>Bu<sub>2</sub>)(CH<sub>2</sub>NEt<sub>2</sub>)Ru(H)(CO)(OH)] in refluxing water for 3 days resulted in the evolution of H<sub>2</sub> with formation of a *cis*-dihydroxo complex. Exposure of this complex to light released O<sub>2</sub> and regenerated the starting hydrido–hydroxo complex. This scheme based on such a simple homogeneous system presents a new idea for the splitting of water. This active complex bears a tridentate PNN pincer ligand, which can donate or accept a proton via a facile dearomatization–aromatization process in cooperation with the metal center.<sup>3</sup> This kind of metal PNN (or PNP) complex has been found to be powerful for many novel reactions,<sup>4</sup> such as dehydrogenative coupling of alcohols with amines to synthesize amides<sup>5</sup> and coupling of alcohols to produce esters,<sup>6</sup> which involves O–H or C–H bond activation. To our knowledge, there has been almost no theoretical work to study these interesting reactions and this kind of metal complex to date. Thus, in this work, we performed detailed density functional theory (DFT) calculations to investigate the energetics and mechanism of thermal H<sub>2</sub> production from water splitting mediated by this Ru(II) PNN complex.

All of the calculations were carried out on a model system (with PMe<sub>2</sub> and NMe<sub>2</sub> groups replacing P<sup>t</sup>Bu<sub>2</sub> and NEt<sub>2</sub> groups) using the B3LYP hybrid functional<sup>7</sup> as implemented in the Gaussian 03 program.<sup>8</sup> The structure of each stationary point was optimized by taking into account bulk solvent (water) effects using the polarizable continuum model (IEF-PCM).<sup>9</sup> Computational details are described in the Supporting Information. We explored the possible pathways for H<sub>2</sub> formation and H<sub>2</sub>O decomposition on the Ru(II) PNN complex and show the most likely one in Scheme 1. The geometrical parameters of the optimized structures are collected in Figure S1. In the starting reactant **1**, a proton on the P side arm can migrate to the hydride ligand, leading to a dihydrogen complex **2**, with dearomatization of the PNN ligand. This step is endergonic by 20.1 kcal/mol and has an activation barrier of 37.6 kcal/mol (Figure 1). The release of H<sub>2</sub> from **2** is endergonic by 6.6 kcal mol<sup>-1</sup>, leading to a coordinatively unsaturated complex **3**. Addition of H<sub>2</sub>O to this vacant site (**3** + H<sub>2</sub>O → **4**) is exergonic by 10.0 kcal/mol. The subsequent cleavage of the O–H bond of H<sub>2</sub>O proceeds by the cooperation of the metal center and the dearomatized PNN ligand, resulting in an aromatic *trans*-dihydroxo complex **5**. This step is exergonic by 11.5 kcal/mol, with a very low barrier of 5.5 kcal/mol. We expected that the *trans*-dihydroxo complex **5** could isomerize to the final main product, the *cis*-dihydroxo complex **8**, but no low-energy pathway was found because of the rigidity of this hexacoordinate complex. However, we noticed that complex **3** can rearrange its ligands to form complex **6**, whose energy is 6.8 kcal/mol lower. The rotation of the ligands must overcome a barrier of 4.4 kcal/mol. Addition of H<sub>2</sub>O to complex **6**

**Scheme 1**



to form complex **7** is exergonic by 8.7 kcal/mol. The subsequent decomposition of H<sub>2</sub>O, accomplished by the metal and the PNN ligand acting in concert, results in the formation of the *cis*-dihydroxo complex **8**. This step is exergonic by 9.6 kcal/mol and has a low barrier of 7.5 kcal/mol. The overall reaction is slightly endergonic by 1.6 kcal/mol, and the highest-activation-barrier step is the heterolytic coupling of the hydride with the captive proton to form H<sub>2</sub>. It is interesting that during the course of this reaction, Ru remains in the 2+ oxidation state.

Comparison with the results calculated in the gas phase shows that water, as the solvent, does not stabilize the intermediates and the transition states. However, the solvent effects increase the energy difference between the main final product **8** and its isomer **5**. In fact, besides this, water can directly participate in the reaction. For instance, addition of a bridging H<sub>2</sub>O molecule as part of the proton-transfer transition state of the rate-limiting step lowers the activation

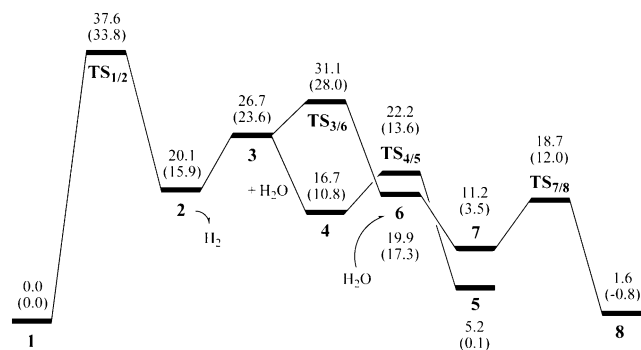


**Figure 1.** Free-energy profile (298 K, in kcal/mol) for H<sub>2</sub> production and H<sub>2</sub>O decomposition on a Ru(II) PNN complex. The energies in the gas phase are also given in parentheses.

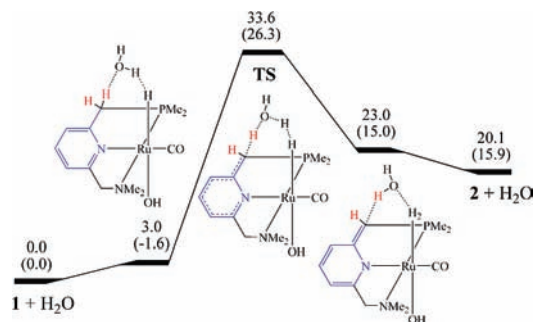


**Figure 2.** Free-energy profile (298 K, in kcal/mol) for addition of a H<sub>2</sub>O bridge as part of the coupling of the Ru-bound hydride with a captive proton.

barrier to 33.6 kcal/mol (Figure 2). Addition of two bridging H<sub>2</sub>O molecules does not further decrease the barrier (see the Supporting Information).

We also explored two other possible pathways for forming H<sub>2</sub>. One was electrophilic attack of the Ru-bound hydride by H<sub>2</sub>O molecule. In the other, the carbonyl group relinquishes the coordination site to H<sub>2</sub>O, after which attack of the binding H<sub>2</sub>O with the hydride ligand occurs in cooperation with the metal center. Both of these processes, which do not involve the PNN ligand, were verified to be unfavorable in energy. The detailed results and discussion are provided in the Supporting Information.

Proton transfer may occur not only between the PNN ligand and the hydride but also between the PNN ligand and the hydroxyl group (Figure 3). This process starts with complex 1', a conformer of 1 in which the hydrogen on the P side arm is closer to the hydroxyl group instead of the hydride. 1' is 1.2 kcal/mol higher in energy than 1. Proton transfer to the hydroxyl group leads to formation of binding water (complex 9). This step is endergonic by 6.6 kcal/mol and has a barrier of 13.6 kcal/mol. Milstein and co-workers reported that this step is endergonic by 5.7 kcal/mol and has a barrier of 15.1 kcal/mol;<sup>2</sup> addition of a water bridge reduces the barrier to 9.3 kcal/mol.<sup>2</sup> The subsequent release of H<sub>2</sub>O from 9 (9 → 10 + H<sub>2</sub>O) is endergonic by 2.1 kcal/mol. If the remaining hydride ligand is transferred to the P side arm as a proton, resulting in aromatic Ru(0) complex 11, an activation barrier of 38.2 kcal/mol must be surmounted. This Ru(0) complex is slightly higher in energy (by 1.9 kcal/mol) than 10 in water.

At this point it is helpful to summarize the whole reaction starting with complex 1. In aromatic complex 1, a proton can be transferred from the PNN ligand to the hydride and also to the hydroxyl group, but the latter process is reversible. On the other hand, once H<sub>2</sub> is formed, it will be released but to be cleaved backward. After H<sub>2</sub> release, the subsequent H<sub>2</sub>O decomposition occurs readily, favorably leading to the *trans*-dihydroxo complex under thermokinetic control. However, the *cis*-dihydroxo complex is still the main final product, as a result of thermodynamic control. Although the overall reaction is slightly endergonic, H<sub>2</sub> escapes from the reaction system into the gas phase at elevated temperatures, driving the reaction to the product side. The rate-limiting step is the formation of H<sub>2</sub>, which has a relatively high activation barrier of 37.6 kcal/mol. However, water can facilitate this step as a bridging molecule. All of these may be the reason why the yield of the final product 8 is 45% while 25% of 1 remains after the reaction proceeds for 3 days at 100 °C.

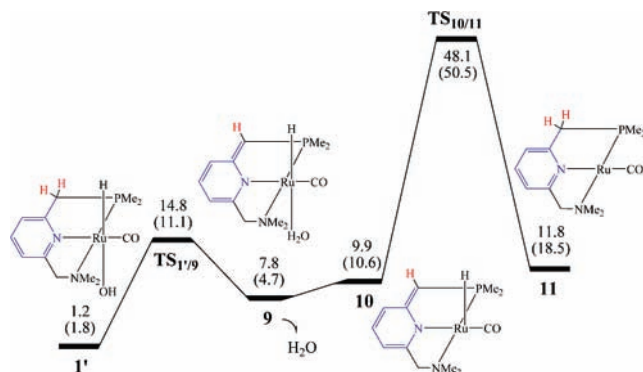


**Figure 3.** Free-energy profile (298 K, in kcal/mol) for transfer of a proton to the hydroxyl group and another back to the side arm.

In conclusion, the molecular mechanism for H<sub>2</sub> production and H<sub>2</sub>O decomposition on an aromatic PNN Ru(II) complex has been elucidated by DFT calculations. An unusual heterolytic coupling of the hydride ligand with a proton that has migrated from the PNN ligand leads to the formation of H<sub>2</sub>, and this coupling is the rate-limiting step for the whole reaction. The metal center and the PNN ligand, which can be dearomatized and aromatized again, play active and synergistic roles in H<sub>2</sub> production and the subsequent H<sub>2</sub>O decomposition. The O–H bond of H<sub>2</sub>O can easily be split via this mechanism. The *cis*-dihydroxo complex is the main final product, and results from thermodynamic control. The evolution of H<sub>2</sub> from the reaction system into the gas phase drives this slightly endergonic reaction to the product side.

**Acknowledgment.** We thank Grants-in-Aid for Scientific Research (18066013, 18GS0207, and 21750063) from the Japan Society for the Promotion of Science, the Kyushu University Global COE Project, the Nanotechnology Support Project, the Joint Project of Chemical Synthesis Core Research Institutions from the Ministry of Culture, Sports, Science, and Technology of Japan (MEXT), and CREST of the Japan Science and Technology Agency.

**Supporting Information Available:** Computational details, optimized geometries of all species, and complete ref.<sup>8</sup> This material is available free of charge via the Internet at <http://pubs.acs.org>.

## References

- (a) Lewis, N. S.; Nocera, D. G. *Proc. Natl. Acad. Sci. U.S.A.* **2006**, *103*, 15729. (b) Barber, J. *Chem. Soc. Rev.* **2009**, *38*, 185.
- Kohl, S. W.; Weiner, L.; Schwartsburd, L.; Konstantinovskii, L.; Shimon, L. J. W.; Ben-David, Y.; Iron, M. A.; Milstein, D. *Science* **2009**, *324*, 74.
- (a) Ben-Ari, E.; Leitius, G.; Shimon, L. J. W.; Milstein, D. *J. Am. Chem. Soc.* **2006**, *128*, 15390. (b) Grützmacher, H. *Angew. Chem., Int. Ed.* **2008**, *47*, 1814.
- (a) Feller, M.; Ben-Ari, E.; Gupta, T.; Shimon, L. J. W.; Leitius, G.; Diskin-Posner, Y.; Weiner, L.; Milstein, D. *Inorg. Chem.* **2007**, *46*, 10479. (b) Kloel, S. M.; Heinekey, D. M.; Goldberg, K. I. *Angew. Chem., Int. Ed.* **2007**, *46*, 4736. (c) Vuzman, D.; Poverenov, E.; Shimon, L. J. W.; Diskin-Posner, Y.; Milstein, D. *Organometallics* **2008**, *27*, 2627.
- Gunanathan, C.; Ben-David, Y.; Milstein, D. *Science* **2007**, *317*, 790.
- Zhang, J.; Leitius, G.; Ben-David, Y.; Milstein, D. *J. Am. Chem. Soc.* **2005**, *127*, 10840.
- Becke, A. D. *J. Chem. Phys.* **1993**, *98*, 5648.
- Frisch, M. J.; et al. *Gaussian 03*, revision D.02; Gaussian, Inc.: Wallingford, CT, 2004.
- (a) Mennucci, B.; Tomasi, J. *J. Chem. Phys.* **1997**, *106*, 5151. (b) Cancès, E.; Mennucci, B.; Tomasi, J. *J. Chem. Phys.* **1997**, *107*, 3032. (c) Tomasi, J.; Mennucci, B.; Cancès, E. *THEOCHEM* **1999**, *464*, 211.

JA905073S